J Nanopart Res (2014) 16:2762
DOI 10.1007/s11051-014-2762-y

RESEARCH PAPER

# Silica-coated ZnS quantum dots as fluorescent probes for the sensitive detection of $Pb^{2+}$ ions

**Hua Qu · Lixin Cao · Ge Su · Wei Liu · Rongjie Gao · Chenghui Xia · Junjie Qin**

Received: 9 October 2014 / Accepted: 14 November 2014 / Published online: 4 December 2014


**Abstract** The silica-coated ZnS quantum dots ($ZnS@SiO_2$ QDs) were prepared via a simple and environmentally friendly process. The oil-soluble ZnS cores were successfully transferred to water by the coating of $SiO_2$ shells. The QDs exhibited satisfying dispersion and luminescent properties in water. The $ZnS@SiO_2$ QDs were directly used as fluorescent probes for heavy metal ions without the addition of any buffer solution. The luminescence of QDs was extremely sensitive to $Pb^{2+}$ ions, and the fluorescence quenching was well described by the Stern–Volmer equation, with an even quenching constant for the $Pb^{2+}$ ions samples concentration ranging from $10^{-9}$ to $2.6 \times 10^{-4}$ M. An extended hypothesis based on the traditional cation exchange mechanism is proposed to analyze the most significant fluorescence quenching effect by $Pb^{2+}$ ions. Studies show that $ZnS@SiO_2$ QDs have great potentials to be a sensor for $Pb^{2+}$ analysis at low to high concentrations.

**Keywords** $ZnS@SiO_2$ · Quantum dot · Fluorescent probe · Detection of $Pb^{2+}$ ions · Sensors

H. Qu · L. Cao (✉) · G. Su · W. Liu · R. Gao · C. Xia · J. Qin
Institute of Material Science and Engineering, Ocean University of China, Qingdao 266100, People's Republic of China
e-mail: caolixin@ouc.edu.cn

H. Qu
Key Laboratory of Marine Environment and Ecology, Ministry of Education, College of Environmental Science and Engineering, Ocean University of China, Qingdao 266100, People's Republic of China

H. Qu
Qingdao Zhongke Institute of Applied Chemistry Technology, Qingdao 266109, People's Republic of China

## Introduction

Heavy metal ions are one type of the most serious contaminants in waters. In recent years, the presence of heavy metals in ambient environment has been sharply increased, owing to the rapid development of modern industry, agriculture and transportation, and in particular the uncontrolled battery manufacturing, metal melting, and old ship demolition (Zhang 2011). Lead (Pb) is a kind of heavy metal with significant environmental and biological toxicities. It is nondegradable in the natural environment for a long time, and is harmful to organisms even at a very low concentration (Rogers et al. 2003). The sensitive detection of heavy metals and successful prevention from damaging effects at the very earliest stage is a proper way to minimize the pollution of heavy metals. Conventional analytical techniques for heavy metals, such as atomic absorption spectrometry, emission spectrometry, chemiluminescence method, X-ray fluorescence spectrometry, stripping voltammetry, and polarography, have been used for the detection

of metal ions for many years. However, most of these techniques suffer the disadvantages of high costs of testing, precise and heavy instruments, and long process for preconcentration and separation of samples, limiting their use in real-time and on-site monitoring of metal ions. So the development of supersensitive, low-cost, and fast methods to detect heavy metal has attracted increasing attention in recent years.

In the last two decades, semiconductor quantum dots (QDs) have attracted much interest due to their outstanding fluorescence properties (Aldana et al. 2001; Jiang et al. 2009; Kanelidis et al. 2011; Lin et al. 2004; Pan et al. 2006), such as broad excitation bands, narrow luminescence peaks, high quantum yields, size- and composition- tunable emission, and high stability against photobleaching (Guo et al. 2003; Mulvihill et al. 2010; Siskova et al. 2011). With the development of techniques in synthesis and surface modification, high-quality QDs have been used to detect a number of substances (Duong and Rhee 2007; Geszke-Moritz et al. 2012; Gan et al. 2012; Zhao et al. 2003). Taking advantage of the rapid fluorescence response, semiconductor QDs are becoming one of the simplest, fastest, and most efficient sensors. Heavy metals in waters usually exist in the form of metallic cations. QD fluorescent probes have shown greater promise for the qualitative and quantitative analysis of heavy metal ions (Ali et al. 2007; Generalova et al. 2011; Koneswaran and Narayanaswamy 2012; Page et al. 2011; Shen et al. 2012; Shete and Benson 2009). Aiming at this application, the QDs should be water-soluble and possess stable fluorescent properties in water. It has been reported the detection of $Cu^{2+}$, $Pb^{2+}$, and $Hg^{2+}$ ions by ZnE and CdE QDs (E = S, Se, or Te) as fluorescent probes. These QDs are mostly coated with organic reagents to improve their water solubility and surface functionalization, and dispersed in buffer solution to obtain stable luminescence in testing.

In this paper, we report the facile synthesis of silica-coated ZnS ($ZnS@SiO_2$) QDs. ZnS is the most environmentally friendly and harmless material in II–VI compounds. Compared with the previous reports that prepared QDs with toxic precursors at high temperature, our strategy is a moderate and green method. So the preparation and application of $ZnS@SiO_2$ QDs will hardly pollute the environment. Subsequently, the $ZnS@SiO_2$ QDs were used as fluorescent probes for detection of heavy metal ions, and they showed fluorescence sensitivity to $Pb^{2+}$ ions. In addition, the luminescence of $ZnS@SiO_2$ QDs is stable in a wide pH range. All these tests were carried out in water without any buffer solution.

## Experiment

### Materials

The zinc acetate dihydrate ($Zn(CH_3COO)_2{\cdot}2H_2O$), oleic acid, tetraethyl orthosilicate (TEOS), triton X-100, *n*-hexanol, and ammonium hydroxide solution ($NH_3{\cdot}H_2O$, 25.0–28.0 %) were purchased from Sinopharm Chemical Reagent CO., Ltd. The sodium oleate was purchased from Shanghai Kefeng Industry CO., Ltd. The sodium sulfide nonahydrate ($Na_2S{\cdot}9H_2O$) was purchased from Beijing Chemical Works. The ethanol and cyclohexane were purchased from Tianjin Bodi Chemical Co., Ltd. All the above reagents were analytical grade and used without further purification.

### Preparation of ZnS, $ZnS@SiO_2$ and $SiO_2$ QDs

The ZnS cores were prepared via a liquid–solid-solution (LSS) process (Wang et al. 2005). Typically, 0.1317 g (0.6 mmol) of $Zn(CH_3COO)_2{\cdot}2H_2O$ and 10 mL of deionized water were added to a 100 mL Teflon cup. A colorless transparent solution was obtained after stirring. Then 15 mL of oleic acid, 2 g of sodium oleate, and 25 mL of ethanol were added into the autoclave in order. The mixture was stirred for 10 min to form a uniform emulsion, and then 10 mL of 0.06 M $Na_2S$ solution was added rapidly. The mixture was stirred for 5 min at room temperature. The Teflon-lined autoclave was sealed tightly and maintained at 200 °C for 12 h, and then cooled to ambient temperature naturally. The product containing ZnS QDs was stored in a well-closed container and used within 1 week.

The $ZnS@SiO_2$ QDs were prepared through the hydrolysis of TEOS in the presence of ZnS cores at room temperature. In a typical synthesis, 1 mL of ZnS product was rinsed with ethanol and cyclohexane to remove the excess oleic acid and other impurities and the ZnS QDs were dispersed in 10 mL of cyclohexane. Then 100 μL of TEOS was injected to ZnS suspension under agitation. After 10 min, 1 mL of triton X-100

and 1 mL of *n*-hexanol were added sequentially and the mixture turned transparent immediately. The mixture was stirred for another 30 min to form the microemulsion system. Then 0.3 mL of $NH_3 \cdot H_2O$ was introduced to initiate the polymerization. After stirring for 24 h, the growth of silica shells completed. The $SiO_2$-coated nanoparticles were separated by centrifugation and washed with ethanol and deionized water. Finally, the ZnS@$SiO_2$ QDs were ultrasonically dispersed in 5 mL of deionized water to form a suspension.

The $SiO_2$ QDs were obtained by the hydrolysis of TEOS using the similar procedure with that of ZnS@$SiO_2$ QDs, except without addition of ZnS QDs as cores.

### Characterization

The ZnS and ZnS@$SiO_2$ QDs were centrifuged and rinsed with cyclohexane/deionized water and ethanol for several times. After drying under vacuum overnight, the powders were obtained for the X-ray powder diffraction (XRD) and Fourier transform infrared spectroscopy (FTIR) examinations. XRD studies were performed with a Rigaku D/max-rB instrument (Cu Kα1 radiation, $\lambda = 1.54060$ Å). FTIR measurements were carried out on a Thermo Fisher Scientific Nicolet 6700 FTIR spectrometer.

Photoluminescence (PL) spectra were recorded on a Jobin Yvon Fluorolog3-P spectrophotometer. All the spectra were monitored at room temperature in ambient atmosphere. The oil-soluble ZnS QDs and water-soluble ZnS@$SiO_2$ QDs were ultrasonically dispersed in cyclohexane and deionized water, respectively, and placed in a 1 cm quartz cuvette for PL measurements. Photomicrographs were obtained from a JEM-1200 EX transmission electron microscope (TEM), using an accelerating voltage of 100 kV. The Zeta potential of ZnS@$SiO_2$ QDs was tested with a Malvern Zetasizer NANO ZS system.

### Detection of metal ions

The suspension of ZnS@$SiO_2$ QDs was ultrasonically dispersed for several minutes before use. In a typical testing, 63 μL of ZnS@$SiO_2$ QDs suspension was added to 2.44 mL of deionized water, and then 10 μL of metal ions solution with a certain concentration was injected to the diluted QDs suspension. The mixture was shaken by hand and left to stand for 10 min, then placed in a quartz cuvette for PL measurements.

## Results and discussion

Figure 1 gives the XRD patterns of ZnS and ZnS@$SiO_2$ QDs. The diffraction peaks at $2\theta = 28.6°$, 47.5°, and 56.3° in curve a could be indexed as the (111), (220), and (311) planes of ZnS in a sphalerite phase (JCPDS Card, File No. 05-0566), while the broad dispersal peaks at about $2\theta = 22°$ in curve b could be attributed to the amorphous $SiO_2$ (Hessel et al. 2006). The characteristic peaks of ZnS are scarcely visible in curve b, which is dissimilar to some earlier reports about silica-coated nanoparticles (Ding et al. 2012; Dong et al. 2009). Although only a small amount of ZnS cores were used in experiments, the existence of them in the final sample is confirmed by the PL results, so the peaks of ZnS are considered to be concealed by the diffraction peaks of abundant $SiO_2$.

Figure 2 shows the TEM images of ZnS and ZnS@$SiO_2$ QDs. From Fig. 2a, it can be seen that the as-prepared ZnS are spherical particles, with a diameter about 6–7 nm. The ZnS QDs show good dispersion stability in cyclohexane, which is the foundation for the growth of $SiO_2$ shells. The TEM images of ZnS@$SiO_2$ QDs are presented in Fig. 2b, c.

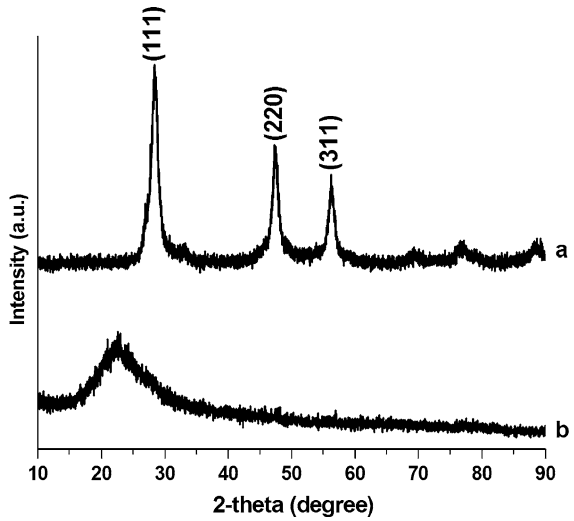


**Fig. 1** Powder XRD patterns of the (*a*) ZnS and (*b*) ZnS@$SiO_2$ QDs

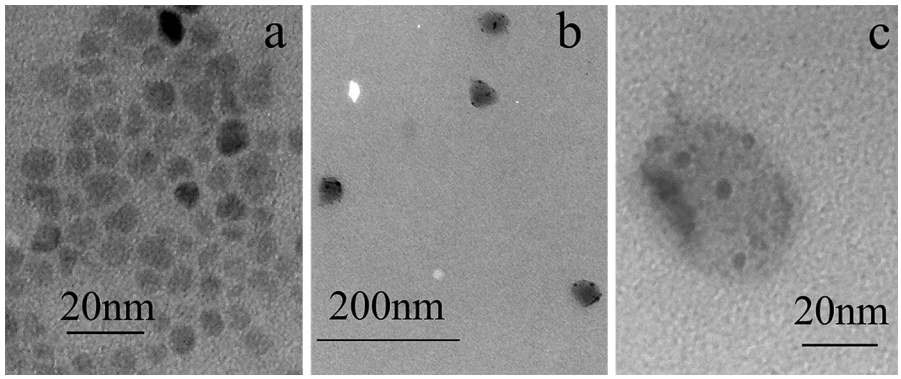


**Fig. 2** TEM images of the **a** ZnS and **b**, **c** ZnS@$SiO_2$ QDs

Each core@shell nanoparticle contains about 5 ZnS cores, and the size of ZnS@$SiO_2$ QDs ranges from 36 to 40 nm. A great effort has been made to obtain the ZnS@$SiO_2$ QDs with single ZnS core, but it has not been fabulously successful to this day. While the good PL performance of samples after being transferred from cyclohexane to water, which is quite different from other reports, may benefit from this imperfect structure.

The FTIR spectra of the bare and silica-coated ZnS QDs are illustrated in Fig. 3. The ZnS QDs were synthesized with oleic acid (OA) as oil phase solvent, and the results confirm the presence of OA ligands on the surface of ZnS QDs. The vibrational band assignment for OA (Siskova et al. 2011) is as follows: The peak at 3,009 $cm^{-1}$ is from O–H stretching vibration and the peak at 2,956 $cm^{-1}$ is assigned to the

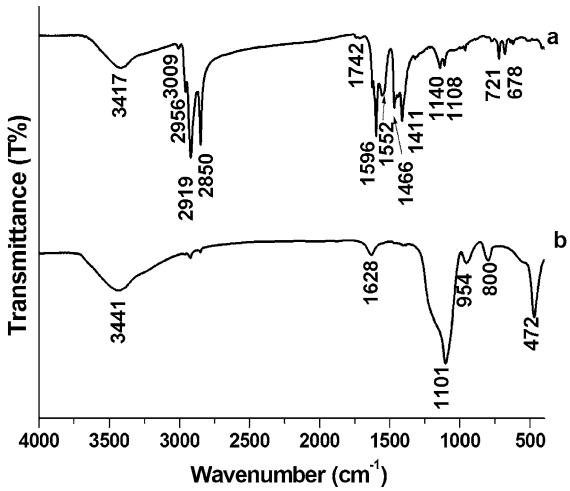


**Fig. 3** FTIR spectra of (*a*) ZnS and (*b*) ZnS@$SiO_2$ QDs

$CH_3$ asymmetric stretching, the peaks at 2,919 and 2,850 $cm^{-1}$ are assigned to the $CH_2$ asymmetric and symmetric stretching, respectively, the peaks at 1742, 1596, and 1552 $cm^{-1}$ originate from C=O stretching vibration, the peak at 1,466 $cm^{-1}$ comes from $CH_3$ asymmetric bending, and the peak at 1,411 is from C–H deformation of $CH_2$ adjacent to C=O, the peak at 721 $cm^{-1}$ generates from the $(CH_2)_7$ in-plane deformations rocking. It is generally known that the QDs modified with OA ligands can be easily dispersed in nonpolar solvents. However, it is quite difficult to transfer them to water and keep steady luminescence performance. For the spectrum of ZnS@$SiO_2$ QDs, the broad -OH peak at 3,441 $cm^{-1}$ indicates that a fraction of the Si atoms exist on the surface has been hydroxylated, which gives the QDs very good dispersion in water. The peak at 1,628 $cm^{-1}$ is ascribed to H–O–H deformation vibration, and the peaks at 1,101 and 800 $cm^{-1}$ are attributed to the Si–O–Si asymmetric and symmetric stretching, respectively. The remaining bands are related to the network bending modes of $SiO_2$ lattice (Jeong et al. 2000; Lee and Wachs 2007).

The emission spectra of ZnS, ZnS@$SiO_2$ and $SiO_2$ QDs are shown in Fig. 4. Excited by 323 nm, the emission spectrum of ZnS QDs shows a peak at about 440 nm. This emission is ascribed to the native trap state emission of ZnS nanocrystals, corresponding to a donor–acceptor type transition (Joo et al. 2003; Murase et al. 1999). Our experimental results on the synthesis of ZnS QDs show a correlation between the emission intensity and the number of sulfur vacancies, so the self-activated centers are suggested to associate with sulfur vacancies, which is correspondent with some classic reporting examples (Becker and Bard

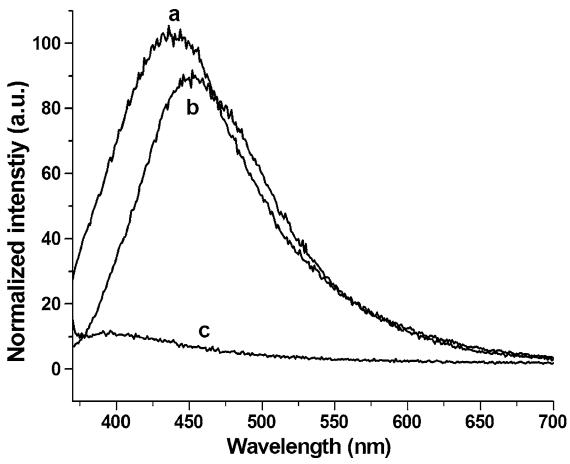


**Fig. 4** Emission spectra of the (*a*) ZnS, (*b*) ZnS@$SiO_2$ and (*c*) $SiO_2$ QDs ($\lambda_{ex}$ = 323 nm)

1983; Karar et al. 2004). While the emission peak of ZnS@$SiO_2$ QDs is at about 450 nm, and the maximum intensity is slightly less than the uncoated sample. It is worthwhile to mention that although the number of ZnS QDs for curve a is theoretically controlled equal to the number of ZnS cores in ZnS@$SiO_2$ QDs for curve b, the latter must be less than the former because of the unavoidable loss during experiments. That is to say, the total ZnS amount in the sample of ZnS@$SiO_2$ is less than in the sample of ZnS QDs. So the emission intensity of ZnS@$SiO_2$ QDs in water is considered to be satisfactory.

Even the $SiO_2$ QDs synthesized under the same conditions are not luminous (curve c), the $SiO_2$ shells play a prominent part in the formation and application of ZnS@$SiO_2$ QDs. First, the oil-soluble ZnS QDs are transferred to water by coating with $SiO_2$ shells, which has been discussed in the discussion of FTIR spectra. Second, the favorable luminescence properties of ZnS@$SiO_2$ QDs are related with $SiO_2$ shells. As is stated above, about 5 ZnS cores are coated in a 36–40 nm sized $SiO_2$ shell. The confinement from core@shell structure may lead to an effect similar to the aggregation of QDs, which cause the red shift of emission peak and the increasement of emission intensity (An et al. 2002; Guo et al. 2014). The ZnS cores are coated with $SiO_2$ to prevent from direct contact with water, so the fluorescence quenching by water could be avoided to some extent. Last but not least, the $SiO_2$ shells have much to do with the tolerance of ZnS@$SiO_2$ for the application as fluorescent probes, which will be elaborated in more detail in the following paragraphs.

Because of the quite good dispersion and luminescent properties in water, ZnS@$SiO_2$ QDs would be expected as fluorescent probes for the detection of heavy metal ions. However, there are some challenges to face in the application of QD fluorescent probes.

First, the water samples in environmental sciences are usually acidic or alkaline, which may greatly influence the luminescence of QDs and even lead to the corrosion of QDs. Dispersing the fluorescent QDs in a buffer solution to keep pH stable at about 7 is an effective method to solve this problem in most cases (Cai et al. 2006; Liang et al. 2010; Liu et al. 2012a, b; Luan et al. 2012). Accordingly, the experimental procedures must be increased and the test cost may be difficult to be reduced. In our study, the luminescence spectra of ZnS@$SiO_2$ QDs with addition of HCl or NaOH in some concentration are shown in Fig. 5a, b, and the changes of PL intensity at 450 nm with dependent on the pH of water samples are presented in Fig. 5c. It is clear that the fluorescence of ZnS@$SiO_2$ QDs is basically stable in the water sample pH range of 3–12. On the one hand, the high endurance of QDs comes from the protection of $SiO_2$ shells, and on the other hand, it may relate with the large volume ratio between QDs systems and test samples. Here the ZnS@$SiO_2$ QDs were dispersed in 2.5 mL deionized water and the volume of water sample is 10 μL. In a word, the ZnS@$SiO_2$ QDs have the potential to be directly used as fluorescent probes for water samples in a broad pH range without the help of buffer solution.

Second, the water samples in environmental generally contain a variety of metal ions, such as alkali metal ions ($Na^+$ and $K^+$), alkaline earth metals ions ($Mg^{2+}$ and $Ca^{2+}$), transition metal ions ($Zn^{2+}$, $Cd^{2+}$, $Mn^{2+}$, $Co^{2+}$, $Fe^{3+}$ and $Cr^{6+}$, etc.), and $Al^{3+}$ which is the most abundant metal ions in crust. Some of them usually quench the emission of QDs. Selectivity is a very important parameter to evaluate the performance of a type of fluorescent probe. In this sense, several environmentally relevant metal ions were chosen to test the specific response of ZnS@$SiO_2$ QDs fluorescence. The PL spectra of ZnS@$SiO_2$ QDs upon addition of 12 common metal ions are shown in Fig. 6a, and the changes of emission intensity at 450 nm are given in Fig. 6b. It can be seen that $Pb^{2+}$ ions induce a prominent fluorescence quenching compared to the blank sample (no metal ion was

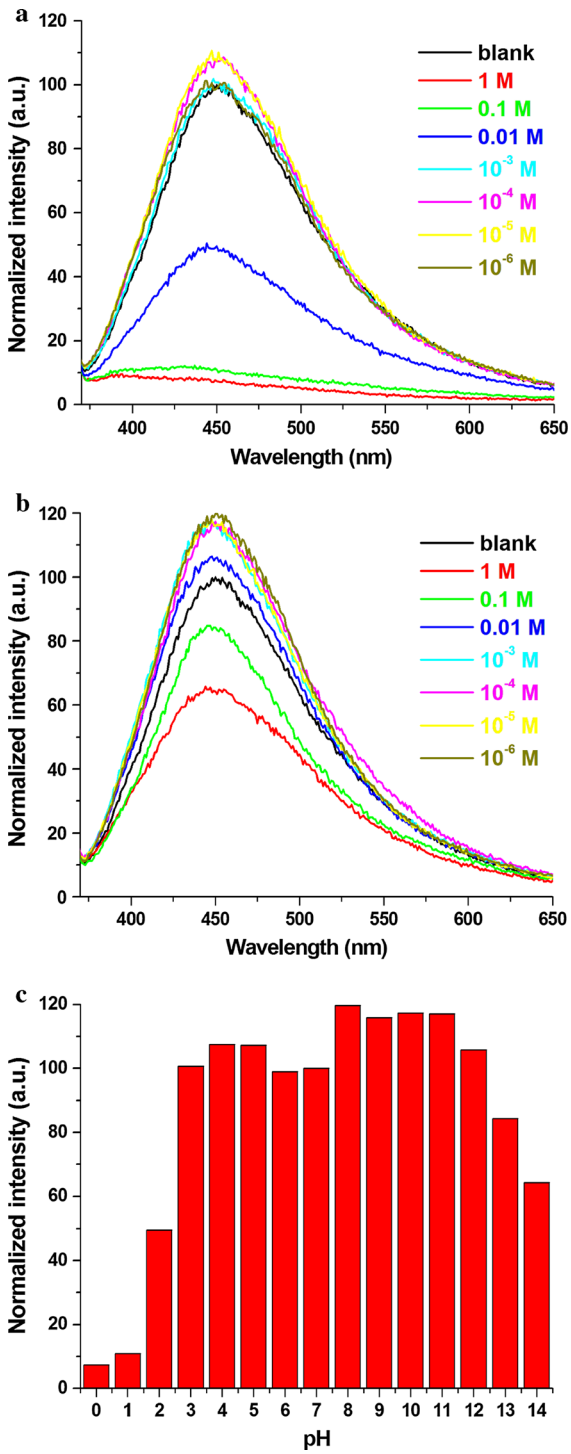


**Fig. 5** PL spectra of $ZnS@SiO_2$ QDs upon addition of different concentrations of **a** HCl and **b** NaOH solution. **c** Emission intensity at 450 nm of PL spectra upon addition of water sample in different pHs ($\lambda_{ex}$ = 323 nm)

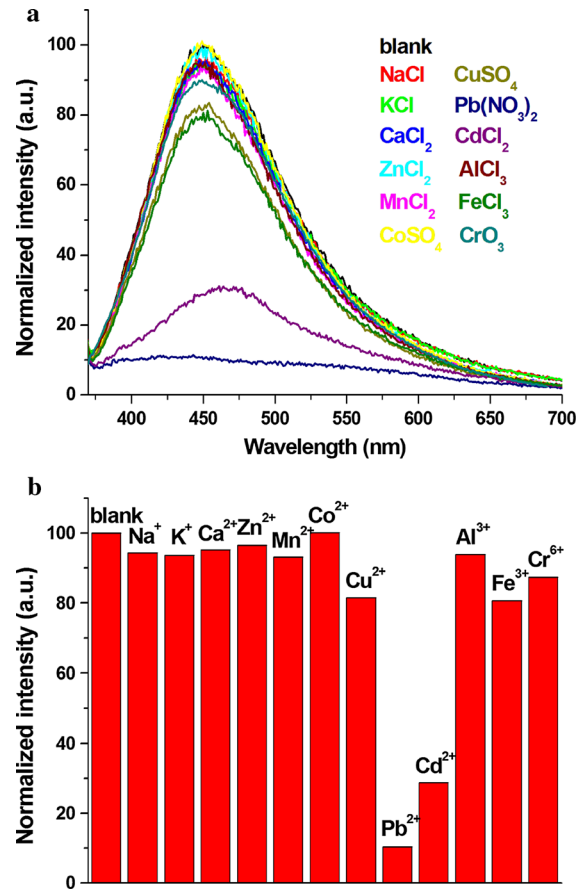


**Fig. 6** **a** PL spectra and **b** emission intensity at 450 nm for $ZnS@SiO_2$ QDs upon addition of different metal ions, respectively. ($\lambda_{ex}$ = 323 nm, concentration of metal ions solution: $10^{-4}$ M)

added), whereas some other metal ions led to slight or even no fluorescence change. Although the luminescence from $ZnS@SiO_2$ QDs is suppressed by $Cd^{2+}$ ions to some extent, the red shift of emission peak is the most obvious characteristic that can distinguish $Cd^{2+}$ ions from $Pb^{2+}$ ions. It can be seen that the $ZnS@SiO_2$ QDs show better selectivity toward $Pb^{2+}$ ions than the other metallic ions, and they may serve as fluorescent sensors for the detection of $Pb^{2+}$ ions in aqueous solution.

Figure 7a illustrates the effect of the different amounts of $Pb^{2+}$ ions on the luminescence spectra of $ZnS@SiO_2$ QDs. The spectra are closely monitored from a very trace concentration ($Pb^{2+}$ ions in water sample: $10^{-9}$ M) until a quite high concentration

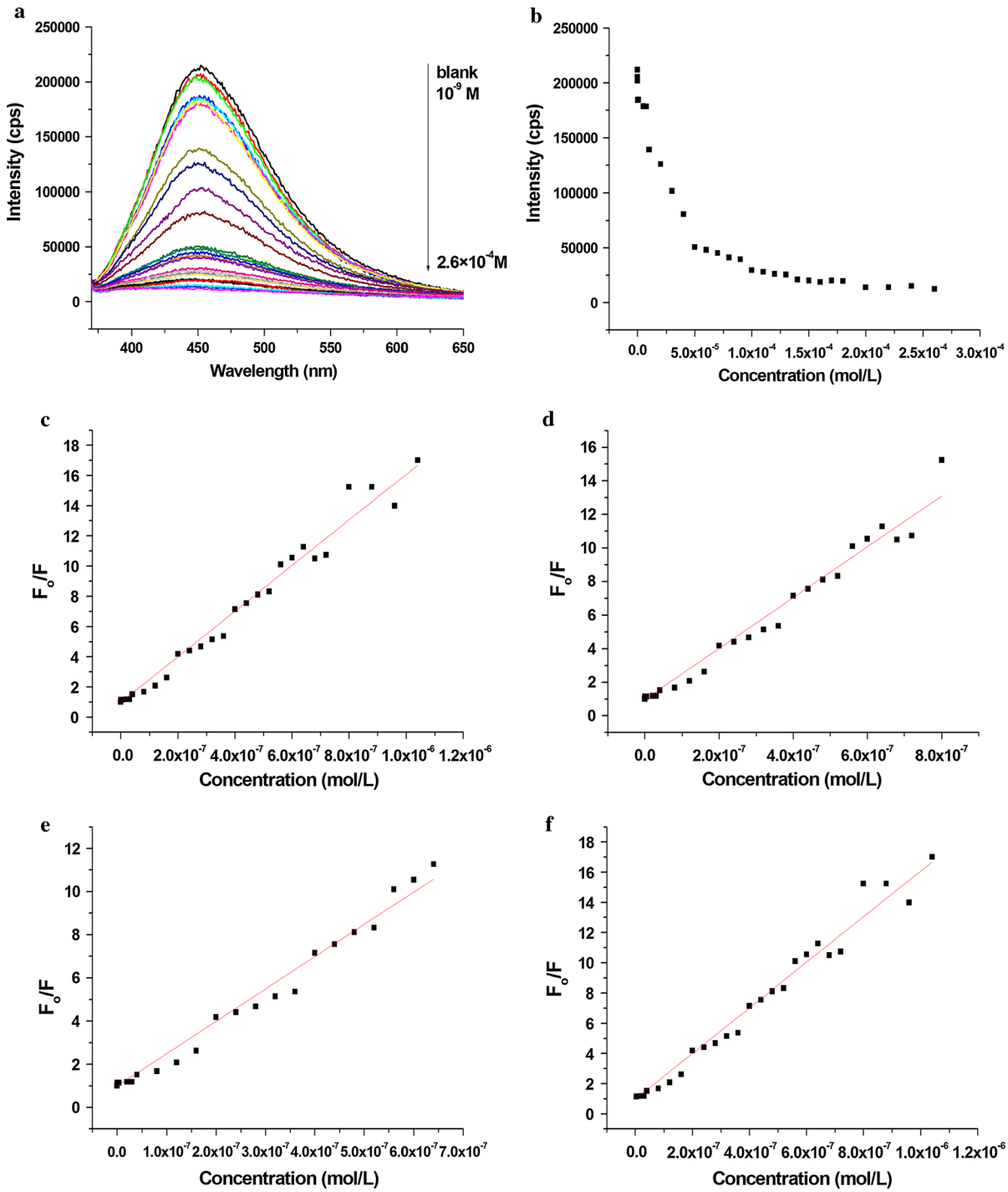


**Fig. 7** **a** PL spectra and **b** fluorescence intensity at 450 nm of $ZnS@SiO_2$ QDs upon addition of $Pb(NO_3)_2$ solution at various concentrations. ($\lambda_{ex} = 323$ nm) (**c**, **d**, **e**, **f**) Stern–Volmer plots representing the quenching effects of $Pb^{2+}$ ions on the fluorescence emission of $ZnS@SiO_2$ QDs at 450 nm

($Pb^{2+}$ ions in water sample: $2.6 \times 10^{-4}$ M). With the increase of $Pb^{2+}$ in water samples added, the fluorescence of ZnS@$SiO_2$ QDs is gradually reduced until completely quenched. The PL intensities at 450 nm corresponding to the $Pb^{2+}$ concentrations in water samples are listed in Fig. 7b. On the whole, all data points follow the hyperbolic distribution. Here we use the Stern–Volmer equation to analyze the PL quenching. The Stern–Volmer equation is a convenient analysis tool for photophysical and photochemical data (Bhalla et al. 2013; Carraway et al. 1991; Chen and Rosenzweig 2002; Gunnlaugsson et al. 2006; Guo et al. 2009; He et al. 2008; Landes et al. 2001). It can describe the dependence of a quenching effect on the concentration of quenchers. In our research, the fluorescence quenching by $Pb^{2+}$ ions is well described by the Stern–Volmer equation

$$F_0/F = 1 + K_{SV}[Q], \quad (1)$$

where $F$ and $F_0$ are the luminescence intensities of ZnS@$SiO_2$ QDs in the presence and absence of $Pb^{2+}$ ions, $K_{SV}$ is the Stern–Volmer constant, and $[Q]$ is the concentration of $Pb^{2+}$ ions in QDs system. It must be noted that the concentration of $Pb^{2+}$ ions in QDs system is only about 0.4 % of that in water samples, which is resulted from the experiment itself. Figure 7c shows the Stern–Volmer plots representing the quenching effects of $Pb^{2+}$ ions on the fluorescence emission of ZnS@$SiO_2$ QDs. A quite good linear relationship between $F_0/F$ and the concentration of $Pb^{2+}$ ions can be observed in the $Pb^{2+}$ concentration range from $4 \times 10^{-12}$ to $1.04 \times 10^{-6}$ M (corresponding to $10^{-9}$ to $2.6 \times 10^{-4}$ M in water samples), and $K_{SV}$ is determined to be $1.51 \times 10^7$ $M^{-1}$ ($R^2 = 0.9794$). The data were analyzed and processed for several times to find the sensitive response range, and the results of data fitting are shown in Fig. 7c–f and listed in Table 1. There are quite little changes in $K_{SV}$ and $R^2$ based on different intervals, implying an even detection sensitive in the whole experimental range. An equation very similar to the Stern–Volmer equation is used to represent the fluorescence quenching by $Pb^{2+}$ ions with greater facility in the potential application

$$F_0/F = 1 + k[Q'], \quad (2)$$

where $k$ is the quenching constant and $[Q']$ is the concentration of $Pb^{2+}$ ions in water samples. The fitting results are also expressed in Table 1.

The wide detection range from $10^{-9}$ to $2.6 \times 10^{-4}$ M made the ZnS@$SiO_2$ QDs-based sensing system competent for $Pb^{2+}$ analysis at low to high concentrations. There was no obvious decrease in the luminescence intensity of ZnS@$SiO_2$ QDs in the experimental condition within 2 h. Furthermore, the fluorescence from ZnS@$SiO_2$ QDs stored as undiluted suspension was with great consistency for longer than 2 months. It is indicated that the ZnS@$SiO_2$ QDs displayed a relative luminescent stability, making them suitable for analytical application.

There are two main types of explanations for the mechanism of fluorescence quenching by heavy metal ions in previous reports. First, the quenching may be caused by the displacement of $Zn^{2+}$ or $Cd^{2+}$ in ZnE or CdE QDs (E = S, Se, or Te) by heavy metal ions (Chan et al. 2010; Liu et al. 2012a, b; Luan et al. 2012; Shen et al. 2012; Sung and Lo 2012; Wang et al. 2011; Yang et al. 2011). It is due to the higher binding affinity to $E^{2-}$ ions and indicated by the lower solubility product constant ($K_{sp}$) than ZnE or CdE. The formed ultrasmall particles of heavy metal sulfides can quench the fluorescence of QDs by facilitating electron–hole nonradiative annihilation (Dong et al. 2006; Isarov and Chrysochoos 1997).

Second, the competitive binding of molecules between QDs and heavy metal ions make the ligands strip from the surface of QDs and sometimes may cause the aggregation of QDs (Ali et al. 2007; Cai et al. 2012; Liang et al. 2010; Wang and Guo 2009; Wang et al. 2012a, b; Wu et al. 2010; Xie et al. 2012). The

**Table 1** The results of data fitting

| [Q] (M) | $K_{SV}$ ($M^{-1}$) | Error | [Q′] (M) | $k$ ($M^{-1}$) | Error | $R^2$ |
|---|---|---|---|---|---|---|
| 0–$10.4 \times 10^{-7}$ | $1.507 \times 10^7$ | $2.783 \times 10^5$ | 0–$2.6 \times 10^{-4}$ | $6.028 \times 10^4$ | 1113 | 0.9794 |
| 0–$8.0 \times 10^{-7}$ | $1.512 \times 10^7$ | $3.377 \times 10^5$ | 0–$2.0 \times 10^{-4}$ | $6.047 \times 10^4$ | 1351 | 0.9739 |
| 0–$6.4 \times 10^{-7}$ | $1.497 \times 10^7$ | $3.027 \times 10^5$ | 0–$1.6 \times 10^{-4}$ | $5.987 \times 10^4$ | 1211 | 0.9819 |
| $4.0 \times 10^{-9}$–$10.4 \times 10^{-7}$ | $1.507 \times 10^7$ | $3.003 \times 10^5$ | $1.0 \times 10^{-6}$–$2.6 \times 10^{-4}$ | $6.028 \times 10^4$ | 1201 | 0.9748 |

QDs are usually capped with some modifiers, such as cysteine, glutathione, and biological molecules etc., containing free $–NH_2$, –COOH, –SH, or some other groups to selectively interact with certain heavy metal ions. It is apparent that the second theory is not applicable here, because the $ZnS@SiO_2$ QDs were directly used without any further surface modification. While the inadaptability of the first theory for our results will be expounded in the following.

The hydroxylated $SiO_2$ shells are negatively charged, which has been affirmed by Zeta potential (−47.6 mV). The free metallic cations can be attracted to surfaces of $SiO_2$ shells by the electrostatic interaction. The $SiO_2$ shells prepared by microemulsion method under the low temperature are generally porous (Darbandi et al. 2007; Shajesh et al. 2009; Xu et al. 2013). It is possible for the metal ions bounded on QDs surface to pass through $SiO_2$ shells and interact with ZnS cores, and the $Zn^{2+}$ ions on the surface of ZnS cores can be exchanged by some metal ions, resulting in a fluorescence response. It is reasonable that the $Cu^{2+}$ ions are more easily deposited than $Pb^{2+}$ ions judging from the solubility product constants ($K_{sp}(CuS) = 6.3 \times 10^{-36}$, $K_{sp}(PbS) = 8.0 \times 10^{-28}$), hence the fluorescence of QDs should be more dramatically quenched by $Cu^{2+}$ ions than by $Pb^{2+}$ ions in accordance with the above first theory. However, the facts are just the opposite. The fluorescence of $ZnS@SiO_2$ QDs is most significantly quenched by $Pb^{2+}$ ions in our study. So here, we propose an extended hypothesis to clarify the problem.

Undoubtedly, there are ultrasmall particles of CuS or PbS formed on the surfaces of ZnS cores. These ultrasmall particles can quench the fluorescence of ZnS cores and act as electron–hole nonradiative recombination centers (Isarov and Chrysochoos 1997). As we all known, ZnS is an important semiconductor materials with a bulk band gap of 3.65 eV, which is the largest value of all II–VI compound semiconductors. CuS and PbS are both narrow gap semiconductors. $Cu_xS$ as bulk material exists in five stable phases at room temperature, with the band gap varying from 1.05 to 1.7 eV and the transitions being direct or indirect (Nascu et al. 1997; Rodriguez-Lazcano et al. 2009). Bulk PbS is a direct band gap semiconductor with a band gap of 0.41 eV (Machol et al. 1993; Wang et al. 1987). Quantum confinement in the QDs results in discrete energy levels and an increase in the effective band gap. The band gap of CuS nanocrystals has been reported to be in the range between 1.25 and 2.81 eV (Mageshwari et al. 2011; Nair et al. 1998; Raevskaya et al. 2004; Yildirim et al. 2009). The band gap of PbS nanocrystals has been reported to be in the range 0.5–2.32 eV (Joshi et al. 2004; Mukherjee et al. 1994; Nanda et al. 2002) and even as high as 5.2 eV (Thielsch et al. 1998). Although the exact band gaps of CuS and PbS ultrafine grains formed on the surface of ZnS cores are unknown, we assume that the electron and hole transfer from the excited ZnS to the energy levels of PbS may be faster than to that of CuS, bringing about the quicker fluorescence quenching by $Pb^{2+}$ ions.

## Conclusions

In summary, we have prepared $ZnS@SiO_2$ QDs by a facile and green process. The ZnS cores were synthesized by a moderate LSS method, and the oil-soluble ZnS QDs were successfully transferred to water through the coating of $SiO_2$ shells. The photoluminescence properties of the core@shell structural nanoparticles were investigated. With the help of $SiO_2$ shells, the $ZnS@SiO_2$ QDs presented an acceptable fluorescence in water, and the luminescence was quite stable after mixing with acidic or alkaline water samples. The QDs were used as fluorescent probes for detection of heavy metal ions without the need for additional buffer solution, and they showed a sensitive fluorescence response to $Pb^{2+}$ ions. The fluorescence quenching was well described by the Stern–Volmer equation, and an even quenching constant was obtained when the $Pb^{2+}$ ions concentration in water samples ranging from $10^{-9}$ to $2.6 \times 10^{-4}$ M. The $ZnS@SiO_2$ QDs are expected to become a potential sensor for $Pb^{2+}$ analysis at low to high concentrations.

**Acknowledgments** This work was supported by the National Natural Science Foundation of China (51172218) and the China Postdoctoral Science Foundation funded project (2013 M541962).

## References

Aldana J, Wang YA, Peng XG (2001) Photochemical instability of CdSe nanocrystals coated by hydrophilic thiols. J Am Chem Soc 123:8844–8850. doi:10.1021/ja016424q

Ali EM, Zheng YG, Yu HH, Ying JY (2007) Ultrasensitive $Pb^{2+}$ detection by glutathione-capped quantum dots. Anal Chem 79:9452–9458. doi:10.1021/ac071074x

An BK, Kwon SK, Jung SD, Park SY (2002) Enhanced emission and its switching in fluorescent organic nanoparticles. J Am Chem Soc 124:14410–14415. doi:10.1021/ja0269082

Becker WG, Bard AJ (1983) Photoluminescence and photoinduced oxygen adsorption of colloidal zinc sulfide dispersions. J Phys Chem 87:4888–4893. doi:10.1021/j150642a026

Bhalla V, Gupta A, Kumar M (2013) A pentacenequinone derivative with aggregation-induced emission enhancement characteristics for the picogram detection of $Fe^{3+}$ ions in mixed aqueous media. Dalton Trans 42:4464–4469. doi:10.1039/c3dt32546f

Cai ZX, Yang H, Zhang Y, Yan XP (2006) Preparation, characterization and evaluation of water-soluble L-cysteine-capped CdS nanoparticles as fluorescence probe for detection of Hg(II) in aqueous solution. Anal Chim Acta 559:234–239. doi:10.1016/j.aca.2005.11.061

Cai ZX, Shi BQ, Zhao L, Ma MH (2012) Ultrasensitive and rapid lead sensing in water based on environmental friendly and high luminescent L-glutathione-capped-ZnSe quantum dots. Spectrochim Acta Part A 97:909–914. doi:10.1016/j.saa.2012.07.069

Carraway ER, Demas JN, Degraff BA (1991) Luminescence quenching mechanism for microheterogeneous systems. Anal Chem 63:332–336. doi:10.1021/ac00004a006

Chan YH, Chen JX, Liu QS, Wark SE, Son DH, Batteas JD (2010) Ultrasensitive copper(II) detection using plasmon-enhanced and photo-brightened luminescence of CdSe quantum dots. Anal Chem 82:3671–3678. doi:10.1021/ac902985p

Chen YF, Rosenzweig Z (2002) Luminescent CdS quantum dots as selective ion probes. Anal Chem 74:5132–5138. doi:10.1021/ac0258251

Darbandi M, Thomann R, Nann T (2007) Hollow silica nanospheres: in situ, semi-in situ, and two-step synthesis. Chem Mater 19:1700–1703. doi:10.1021/cm062803c

Ding HL, Zhang YX, Wang S, Xu JM, Xu SC, Li GH (2012) $Fe_3O_4$@$SiO_2$ core/shell nanoparticles: the silica coating regulations with a single core for different core sizes and shell thicknesses. Chem Mater 24:4572–4580. doi:10.1021/cm302828d

Dong CQ, Qian HF, Fang NH, Ren JC (2006) Study of fluorescence quenching and dialysis process of CdTe quantum dots, using ensemble techniques and fluorescence correlation spectroscopy. J Phys Chem B 110:11069–11075. doi:10.1021/jp060279r

Dong BH, Cao LX, Su G, Liu W, Qu H, Jiang DX (2009) Synthesis and characterization of the water-soluble silica-coated ZnS:Mn nanoparticles as fluorescent sensor for $Cu^{2+}$ ions. J Colloid Interface Sci 339:78–82. doi:10.1016/j.jcis.2009.07.039

Duong HD, Rhee JI (2007) Use of CdSe/ZnS core-shell quantum dots as energy transfer donors in sensing glucose. Talanta 73:899–905. doi:10.1016/j.talanta.2007.05.011

Gan TT, Zhang YJ, Zhao NJ, Xiao X, Yin GF, Yu SH, Wang HB, Duan JB, Shi CY, Liu WQ (2012) Hydrothermal synthetic mercaptopropionic acid stabled CdTe quantum dots as fluorescent probes for detection of $Ag^{+}$. Spectrochim Acta Part A 99:62–68. doi:10.1016/j.saa.2012.09.005

Generalova AN, Oleinikov VA, Zarifullina MM, Lankina EV, Sizova SV, Artemyev MV, Zubov VP (2011) Optical sensing quantum dot-labeled polyacrolein particles prepared by layer-by-layer deposition technique. J Colloid Interface Sci 357:265–272. doi:10.1016/j.jcis.2011.02.002

Geszke-Moritz M, Clavier G, Lulek J, Schneider R (2012) Copper- or manganese-doped ZnS quantum dots as fluorescent probes for detecting folic acid in aqueous media. J Lumin 132:987–991. doi:10.1016/j.jlumin.2011.12.014

Gunnlaugsson T, Glynn M, Tocci (nee Hussey) GM, Kruger PE, Pfeffer FM (2006) Anion recognition and sensing in organic and aqueous media using luminescent and colorimetric sensors. Coord Chem Rev 250:3094–3117. doi:10.1016/j.ccr.2006.08.017

Guo WZ, Li JJ, Wang YA, Peng XG (2003) Luminescent CdSe/CdS core/shell nanocrystals in dendron boxes: superior chemical, photochemical and thermal stability. J Am Chem Soc 125:3901–3909. doi:10.1021/ja028469c

Guo WW, Yuan JP, Wang EK (2009) Oligonucleotide-stabilized Ag nanoclusters as novel fluorescence probes for the highly selective and sensitive detection of the $Hg^{2+}$ ion. Chem Commun 45:3395–3397. doi:10.1039/b821518a

Guo JJ, Zhang Y, Luo YL, Shen F, Sun CY (2014) Efficient fluorescence resonance energy transfer between oppositely charged CdTe quantum dots and gold nanoparticles for turn-on fluorescence detection of glyphosate. Talanta 125:385–392. doi:10.1016/j.talanta.2014.03.033

He Y, Wang HF, Yan XP (2008) Exploring Mn-doped ZnS quantum dots for the room-temperature phosphorescence detection of enoxacin in biological fluids. Anal Chem 80:3832–3837. doi:10.1021/ac800100y

Hessel CM, Henderson EJ, Veinot JGC (2006) Hydrogen silsesquioxane: a molecular precursor for nanocrystalline Si–$SiO_2$ composites and freestanding hydride-surface-terminated silicon nanoparticles. Chem Mater 18:6139–6146. doi:10.1021/cm0602803

Isarov AV, Chrysochoos J (1997) Optical and photochemical properties of nonstoichiometric cadmium sulfide nanoparticles: surface modification with copper(II) ions. Langmuir 13:3142–3149. doi:10.1021/la960985r

Jeong AY, Koo SM, Kim DP (2000) Characterization of hydrophobic $SiO_2$ powders prepared by surface modification on wet gel. J Sol-Gel Sci Technol 19:483–487. doi:10.1023/a:1008716017567

Jiang DX, Cao LX, Su G, Liu W, Qu H, Sun YG, Dong BH (2009) Synthesis and luminescence properties of ZnS:Mn/ZnS core/shell nanorod structures. J Mater Sci 44:2792–2795. doi:10.1007/s10853-009-3367-1

Joo J, Na HB, Yu T, Yu JH, Kim YW, Wu FX, Zhang JZ, Hyeon T (2003) Generalized and facile synthesis of semiconducting metal sulfide nanocrystals. J Am Chem Soc 125:11100–11105. doi:10.1021/ja0357902

Joshi RK, Kanjilal A, Sehgal HK (2004) Solution grown PbS nanoparticle films. Appl Surf Sci 221:43–47. doi:10.1016/S0169-4332(03)00955-3

Kanelidis I, Vaneski A, Lenkeit D, Pelz S, Elsner V, Stewart RM, Rodriguez-Fernandez J, Lutich AZ, Susha AS, Theissmann R, Adamczyk S, Rogach AL, Holder E (2011) Inorganic–organic nanocomposites of CdSe nanocrystals surface-modified with oligo- and poly(fluorene) moieties. J Mater Chem 21:2656–2662. doi:10.1039/c0jm03546g

Karar N, Singh F, Mehta BR (2004) Structure and photoluminescence studies on ZnS:Mn nanoparticles. J Appl Phys 95:656–660. doi:10.1063/1.1633347

Koneswaran M, Narayanaswamy R (2012) CdS/ZnS core–shell quantum dots capped with mercaptoacetic acid as fluorescent probes for Hg(II) ions. Microchim Acta 178:171–178. doi:10.1007/s00604-012-0819-0

Landes C, Burda C, Braun M, El-Sayed MA (2001) Photoluminescence of CdSe nanoparticles in the presence of a hole acceptor: n-butylamine. J Phys Chem B 105:2981–2986. doi:10.1021/jp0041050

Lee EL, Wachs IE (2007) In situ spectroscopic investigation of the molecular and electronic structures of $SiO_2$ supported surface metal oxides. J Phys Chem C 111:14410–14425. doi:10.1021/jp0735482

Liang GX, Liu HY, Zhang JR, Zhu JJ (2010) Ultrasensitive $Cu^{2+}$ sensing by near-infrared-emitting CdSeTe alloyed quantum dots. Talanta 80:2172–2176. doi:10.1016/j.talanta.2009.11.025

Lin Y, Zhang J, Kumacheva E, Sargent EH (2004) Third-order optical nonlinearity and figure of merit of CdS nanocrystals chemically stabilized in spin-processable polymeric films. J Mater Sci 39:993–996. doi:10.1023/b:jmsc.0000012932.23656.a9

Liu BY, Zeng F, Wu GF, Wu SZ (2012a) Nanoparticles as scaffolds for FRET-based ratiometric detection of mercury ions in water with QDs as donors. Analyst 137:3717–3724. doi:10.1039/c2an35434a

Liu ZQ, Liu SP, Yin PF, He YQ (2012b) Fluorescence enhancement of CdTe/CdS quantum dots by coupling of glyphosate and its application for sensitive detection of copper ion. Anal Chim Acta 745:78–84. doi:10.1016/j.aca.2012.07.033

Luan WL, Yang HW, Wan Z, Yuan BX, Yu XH, Tu ST (2012) Mercaptopropionic acid capped CdSe/ZnS quantum dots as fluorescence probe for lead(II). J Nanopart Res 14:762–769. doi:10.1007/s11051-012-0762-3

Machol JL, Wise FW, Patel RC, Tanner DB (1993) Vibronic quantum beats in PbS microcrystallites. Phys Rev B 48:2819–2822. doi:10.1103/physrevb.48.2819

Mageshwari K, Mali SS, Hemalatha T, Sathyamoorthy R, Patil PS (2011) Low temperature growth of CuS nanoparticles by reflux condensation method. Prog Solid State Chem 39:108–113. doi:10.1016/j.progsolidstchem.2011.10.003

Mukherjee M, Datta A, Chakravorty D (1994) Electrical resistivity of nanocrystalline PbS grown in a polymer matrix. Appl Phys Lett 64:1159–1161. doi:10.1063/1.110838

Mulvihill MJ, Habas SE, Plante IJL, Wan JM, Mokari T (2010) Influence of size, shape, and surface coating on the stability of aqueous suspensions of CdSe nanoparticles. Chem Mater 22:5251–5257. doi:10.1021/cm101262s

Murase N, Jagannathan R, Kanematsu Y, Watanabe M, Kurita A, Hirata K, Yazawa T, Kushida T (1999) Fluorescence and EPR characteristics of $Mn^{2+}$-doped ZnS nanocrystals prepared by aqueous colloidal method. J Phys Chem B 103:754–760. doi:10.1021/jp9828179

Nair MTS, Guerrero L, Nair PK (1998) Conversion of chemically deposited CuS thin films to $Cu_{1.8}S$ and $Cu_{1.96}S$ by annealing. Semicond Sci Technol 13:1164–1169. doi:10.1088/0268-1242/13/10/019

Nanda KK, Kruis FE, Fissan H, Acet M (2002) Band-gap tuning of PbS nanoparticles by in-flight sintering of size classified aerosols. J Appl Phys 91:2315–2321. doi:10.1063/1.1431429

Nascu C, Pop I, Ionescu V, Indrea E, Bratu I (1997) Spray pyrolysis deposition of CuS thin films. Mater Lett 32:73–77. doi:10.1016/s0167-577x(97)00015-3

Page LE, Zhang X, Jawaid AM, Snee PT (2011) Detection of toxic mercury ions using a ratiometric CdSe/ZnS nanocrystal sensor. Chem Commun 47:7773–7775. doi:10.1039/c1cc11442e

Pan DC, Wang Q, Pang JB, Jiang SC, Ji XL, An LJ (2006) Semiconductor "nano-onions" with multifold alternating CdS/CdSe or CdSe/CdS structure. Chem Mater 18:4253–4258. doi:10.1021/cm0601032

Raevskaya AE, Stroyuk AL, Kuchmii SY, Kryukov AI (2004) Catalytic activity of CuS nanoparticles in hydrosulfide ions air oxidation. J Mol Catal A Chem 212:259–265. doi:10.1016/j.molcata.2003.11.010

Rodriguez-Lazcano Y, Martinez H, Calixto-Rodriguez M, Rodriguez AN (2009) Properties of CuS thin films treated in air plasma. Thin Solid Films 517:5951–5955. doi:10.1016/j.tsf.2009.03.075

Rogers JT, Richards JG, Wood CM (2003) Ionoregulatory disruption as the acute toxic mechanism for lead in the rainbow trout (oncorhynchus mykiss). Aquat Toxicol 64:215–234. doi:10.1016/s0166-445x(03)00053-5

Shajesh P, Smitha S, Aravind PR, Warrier KGK (2009) Synthesis, structure and properties of cross-linked $R(SiO_{1.5})/SiO_2$ (R = 3-glycidoxypropyl) porous organic inorganic hybrid networks dried at ambient pressure. J Colloid Interface Sci 336:691–697. doi:10.1016/j.jcis.2009.04.023

Shen YY, Li LL, Lu Q, Ji J, Fei R, Zhang JR, Abdel-Halim ES, Zhu JJ (2012) Microwave-assisted synthesis of highly luminescent CdSeTe@ZnS–$SiO_2$ quantum dots and their application in the detection of Cu(II). Chem Commun 48:2222–2224. doi:10.1039/c2cc16329b

Shete VS, Benson DE (2009) Protein design provides lead(II) ion biosensors for imaging molecular fluxes around red blood cells. Biochemistry 48:462–470. doi:10.1021/bi801777h

Siskova K, Kubala M, Dallas P, Jancik D, Thorel A, Ilik P, Zboril R (2011) The effect of surface modification on the fluorescence and morphology of CdSe nanoparticles embedded in a 3D phosphazene-based matrix: nanowire-like quantum dots. J Mater Chem 21:1086–1093. doi:10.1039/c0jm02360d

Sung TW, Lo YL (2012) Highly sensitive and selective sensor based on silica-coated CdSe/ZnS nanoparticles for $Cu^{2+}$ ion detection. Sens Actuators B 165:119–125. doi:10.1016/j.snb.2012.02.028

Thielsch R, Bohme T, Reiche R, Schlafer D, Bauer HD, Bottcher H (1998) Quantum-size effects of PbS nanocrystallites in evaporated composite films. Nanostruct Mater 10:131–149. doi:10.1016/S0965-9773(98)00056-7

Wang X, Guo XQ (2009) Ultrasensitive $Pb^{2+}$ detection based on fluorescence resonance energy transfer (FRET) between quantum dots and gold nanoparticles. Analyst 134:1348–1354. doi:10.1039/b822744f

Wang Y, Suna A, Mahler W, Kasowski R (1987) PbS in polymers. From molecules to bulk solids. J Chem Phys 87:7315–7322. doi:10.1063/1.453325

Wang X, Zhuang J, Peng Q, Li YD (2005) A general strategy for nanocrystal synthesis. Nature 437:121–124. doi:10.1038/nature03968

Wang HG, Sun L, Li YP, Fei XL, Sun MD, Zhang CQ, Li YX, Yang QB (2011) Layer-by-layer assembled $Fe_3O_4$@-C@CdTe core/shell microspheres as separable luminescent probe for sensitive sensing of $Cu^{2+}$ ions. Langmuir 27:11609–11615. doi:10.1021/la202295b

Wang HY, Chen QF, Tan ZA, Yin XX, Wang L (2012a) Electrochemiluminescence of CdTe quantum dots capped with glutathione and thioglycolic acid and its sensing of $Pb^{2+}$. Electrochim Acta 72:28–31. doi:10.1016/j.electacta.2012.03.146

Wang YQ, Liu Y, He XW, Li WY, Zhang YK (2012b) Highly sensitive synchronous fluorescence determination of mercury (II) based on the denatured ovalbumin coated CdTe QD. Talanta 99:69–74. doi:10.1016/j.talanta.2012.04.064

Wu CS, Oo MKK, Fan XD (2010) Highly sensitive multiplexed heavy metal detection using quantum-dot-labeled DNAaymes. ACS Nano 4:5897–5904. doi:10.1021/nn1021988

Xie WY, Huang WT, Luo HQ, Li NB (2012) CTAB-capped Mn-doped ZnS quantum dots and label-free aptamer for room-temperature phosphorescence detection of mercury ions. Analyst 137:4651–4653. doi:10.1039/c2an35777a

Xu ZH, Yu JG, Liu G, Cheng B, Zhou P, Li XY (2013) Microemulsion-assisted synthesis of hierarchical porous $Ni(OH)_2/SiO_2$ composites toward efficient removal of formaldehyde in air. Dalton Trans 42:10190–10197. doi:10.1039/c3dt51067k

Yang FP, Ma Q, Yu W, Su XG (2011) Naked-eye colorimetric analysis of $Hg^{2+}$ with bi-color CdTe quantum dots multilayer films. Talanta 84:411–415. doi:10.1016/j.talanta.2011.01.054

Yildirim MA, Ates A, Astam A (2009) Annealing and light effect on structural, optical and electrical properties of CuS, CuZnS and ZnS thin films grown by the SILAR method. Physica E 41:1365–1372. doi:10.1016/j.physe.2009.04.014

Zhang DJ (2011) Heavy metals hazards and food safety. People's Medical Publishing House, Beijing

Zhao XJ, Tapec-Dytioco R, Tan WH (2003) Ultrasensitive DNA detection using highly fluorescent bioconjugated nanoparticles. J Am Chem Soc 125:11474–11475. doi:10.1021/ja0358854